RSC Advances

PAPER

View Article Online
View Journal | View Issue

Cite this: *RSC Adv.*, 2014, **4**, 8138

Bioinspired superhydrophobic surfaces with directional Adhesion†

Jiale Yong, Qing Yang, Feng Chen,* Dongshi Zhang, Guangqing Du, Hao Bian, Jinhai Si and Xun Hou

Received 22nd November 2013
Accepted 10th January 2014

DOI: 10.1039/c3ra46929h

www.rsc.org/advances

Butterfly wings have the ability to directionally control the movement of water microdroplets. However, the realization of artificial directional sliding biosurfaces has remained challenging. Inspired by butterfly wings, a new kind of directional patterned surface is developed to achieve superhydrophobicity and anisotropic adhesive properties at the one-dimensional level. The surface is composed of a hydrophobic triangle array and surrounding superhydrophobic structure. On the as-prepared surface, a droplet rolls along one direction distinctly easier than its opposite direction. The maximum anisotropy of sliding angles along two opposite directions can reach 21°. This unique ability is ascribed to the direction-dependent arrangement of the two-dimensional (2D) triangle array patterns. The directional adhesive superhydrophobic surfaces could be potentially applied in novel microfluid-controllable devices and directional easy-cleaning coatings.

1. Introduction

Anisotropic microstructured surfaces allow water striders to walk on water,[1,2] butterflies to shed water droplet from their wings,[3] and cactus and spider silk to collect fog.[4,5] Capturing these natural features in biomimetic surfaces is an active area of research.[6–9] In nature, it is well known that the sliding angle (SA) values are different for a water droplet rolling along two vertical directions on the surface of a rice leaf.[10] This unique property is based on the arrangement of the microstructures of the rice leaf. The microscale papillas are arranged in one-dimensional order parallel to the leaf edge and randomly in the other directions.[11,12] In fact, the anisotropy of rice leaf is defined at the two-dimensional (2D) level. Recent researches have shown directional adhesion (at the one-dimensional level) on the superhydrophobic butterfly wings.[3,6] A droplet easily rolls off the surface of the wings along the radial outward (RO) direction of the central axis of the body, but is pinned tightly against the RO direction. Anisotropic superhydrophobic surfaces are attracting considerable attention for their competence of driving liquid flow along a desired direction, enabling their potential applications in microfluidics and lab-on-chip systems.[13–15] Therefore, many efforts have been made in developing an artificial superhydrophobic surface with anisotropic adhesion in the past several years. Compared with the numerous rice leaf-inspired anisotropic superhydrophobic surfaces which are usually prepared by 2D level micro-patterns, such as grooves,[11,16–18] the fabrication of anisotropic superhydrophobic surfaces with directional adhesion is becoming an active research subject until recent years. For example, Tseng *et al.* presented water droplets that undergo spontaneous self-directed motion upon contact with a chemically patterned nanotextured surface with wedge-shaped gradient.[19] But for this spatial gradient-based fluidic pathway, droplet motion occurs over a limited range before sticking occurs. Demirel *et al.* prepared an engineered nanofilm, composed of an array of oblique angle poly nanorods, which demonstrates directional sliding behaviour by means of a pin-release droplet ratchet mechanism.[20] Zheng *et al.* reported a novel taper-ratchet array on ryegrass leaf with effective directional water shedding-off properties.[21] By a couple of replication operations, the polymer surfaces are fabricated successfully from ryegrass leaf, displaying a robust property of directional water shedding-off. However, the above-mentioned surfaces are in fact 3D structures. To best of our knowledge, successful fabrication of artificial superhydrophobic surfaces with different adhesion along the opposite directions (at the one-dimensional level) like butterfly wings *via* the flat 2D patterns has still not been demonstrated.

Up to now, many techniques have been adopted to produce superhydrophobic surfaces and anisotropic wetting surfaces, including self-assembly, electrospinning, plasma-treated surfaces, lithography, wet chemical processes, and laser etching.[22–26] Among these techniques, micromachining by femtosecond (fs) laser is particularly attractive from the perspectives of negligible heat-affected zone, precise ablation threshold and high resolution.[27–30] The fs laser can not only

State Key Laboratory for Manufacturing System Engineering & Key Laboratory of Photonics Technology for Information of Shaanxi Province, School of Electronics & Information Engineering, Xi'an Jiaotong University, Xi'an, 710049, P.R. China. E-mail: chenfeng@mail.xjtu.edu.cn

† Electronic supplementary information (ESI) available: Movies S1, S2, S3 and S4. See DOI: 10.1039/c3ra46929h

produce the topography with two scale roughness *via* a one-step process, but can also be applied to a wide variety of materials such as metals, glasses, ceramics and polymers.[31–33] In combination with a precise three-dimensional computer number control translation stage, fs laser micromachining provides a quick and efficient prototyping means which can control the processing position precisely being independent of expensive masks and clean room. A wide variety of patterns can be realized, exhibiting unique wetting property.[34–36] Therefore, the fs laser has been extensively applied to the modulation of surface wettability.

In this paper, we present a facile patterned surface, inspired by butterfly wings, to realize superhydrophobicity and directional adhesion that a droplet rolls along one direction easier than its opposite direction. The surface is composed of hydrophobic triangle array and surrounding superhydrophobic structure. The base length and vertex angle of the triangle array pattern have important effect on the superhydrophobicity and anisotropy of the as-prepared surfaces. The anisotropy is obtained just when the droplets have close size with a single hydrophobic triangle. The maximum difference of the SAs along two opposite directions can reach 21°. This unique ability is ascribed to the direction-dependent arrangement of triangle array patterns.

2. Experimental Section

2.1. Material

Polydimethylsiloxane (PDMS) is an intrinsic hydrophobic material, widely used in biomedicine field and lab-on-chip devices. In the current investigation, the PDMS thin films were generally prepared from a 10 : 1 mixture (by weight) of prepolymer (DC-184A, Dow Corning Corporation) and curing agent (DC-184B, Dow Corning Corporation), poured onto a clean glass plate and kept there for 10 min in a vacuum desiccator, so that the trapped air bubbles could emerge to the surface. After removing all the air bubbles, the mixture was solidified in an oven at 100 °C for 2 hours. The solidified PDMS samples were carefully peeled off from the glass plate, and then rinsed with deionized water with sonication.

2.2. Structured patterns

Fig. 1 shows the schematic illustration of configurations used to fabricate triangle array patterns on PDMS films. The gray domain denotes the fs laser irradiated region. After fs laser irradiation, the unstructured domain turns out to be a triangle array pattern (the white domain). Each isosceles triangle has a base length of d and a vertex angle of α. By adjusting the d and α, the size and shape of the triangle array can be modulated as well as the wettability. In addition, the 1 and 2 directions, which parallel to the symmetry axis of isosceles triangles, are defined in Fig. 1.

2.3. Surface laser irradiation

The micro/nanoscale hierarchical rough structure (the gray domain in Fig. 1) was fabricated by fs laser irradiation in ambient conditions on flat PDMS surface. The schematic of the experimental setup was shown in our previous work.[17,28,31,32,34–36] The PDMS samples were mounted on a motorized *x-y-z* translation stage controlled by a computer and positioned perpendicularly to the direction of laser incidence, and then irradiated by a regenerative amplified Ti:sapphire laser system (CoHerent, Libra-usp-1K-he-200) with a center wavelength of 800 nm which could afford 50 fs pulses at a repetition rate of 1 kHz. The Gaussian laser beam was focused by a microscope objective lens (10×, NA = 0.30, Nikon) on the samples. A mechanical shutter was used as a switch to turn on and off the laser beam. In the experiment, a line-by-line and serial scanning process was used. Each sample was fabricated with a constant average power of 30 mW at a scanning speed of 4 mm s^{-1}, and the interval of adjacent laser scanning lines was held constant at 4 μm. Following the irradiation process, the samples were cleaned by deionized water in ultrasonic bath at room temperature for 10 minutes.

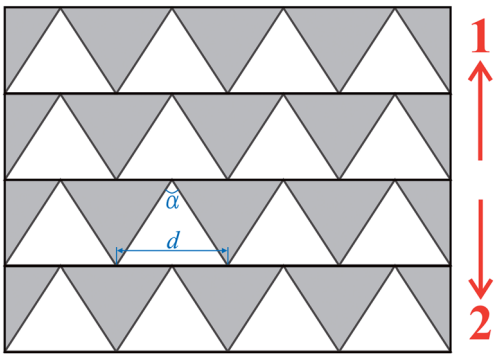

Fig. 1 Schematic illustration of the fabrication of triangle array patterns. The gray domain is irradiated by a femtosecond laser and shows micro/nanoscale hierarchical rough structure. The white domain is intrinsic smooth surface which is not irradiated by femtosecond laser and forms a triangle array.

2.4. Morphology analysis and contact/sliding angle characterization

The morphology of the as-prepared surfaces irradiated by a fs laser was characterized by a JSM-7000F scanning electron microscopy (SEM, JEOL, Japan). The water contact angles (CAs) and the SAs of 7 μl water droplets on the surface were measured by a JC2000D4 contact-angle system (POWEREACH, China) at ambient temperature, using a sessile drop method. The average values were obtained by measuring five different points on the same surface.

3. Results and discussion

Fig. 2a and b show the SEM images of the as-prepared PDMS surfaces consisting of periodic triangle arrays. The intrinsic or untreated PDMS surface is smooth (Fig. 2c) and shows ordinary hydrophobicity with a water CA of 110° ± 1.5° (Fig. 2e). Fig. 2d shows that the fs laser structured region is characterized by an irregular rough structure of an order of micrometer decorating

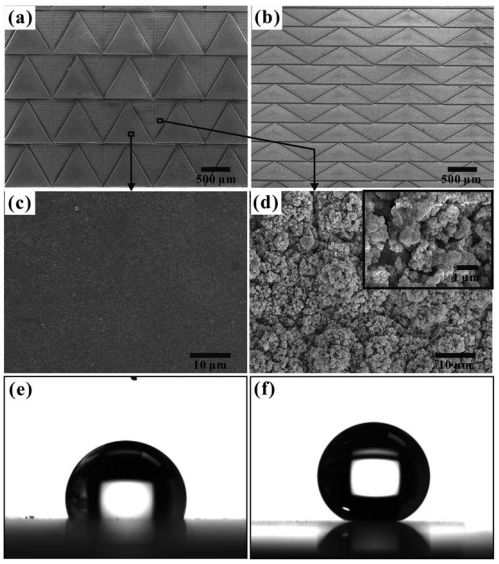

Fig. 2 (a and b) SEM images of as-prepared triangle array patterns with different shapes. (c and d) Large magnification SEM images of the non-irradiated and laser-induced domains, respectively. (e and f) The shapes of a 7 μl water droplet on untreated (e) and completely rough (f) PDMS surfaces, respectively.

with tens or hundreds of nm nanostructures. The micro/nanometer binary structures can trap a large amount of air, which is helpful to give rise to superhydrophobicity.[31,33,35,36] After fs laser scanning, the static CA on the completely rough surface is as high as 157° ± 0.5° (Fig. 2f), even without any modification by materials of low surface energy. In addition, the completely rough surface shows ultralow and isotropic water adhesion because the droplet is very difficult to land on the surface, and the SAs in all directions are lower than 1° (see Movie S1 in the ESI†). Therefore, the triangle array patterned structure is a heterogeneous topographic surface including both superhydrophobic and ordinary hydrophobic domains.

Anisotropic wetting and dewetting are very important properties on the heterogeneity or heterogeneous topographic patterned surfaces. The static and dynamic wettability of the triangle array pattern with d of 1200 μm and α of 60° are shown in Fig. 3. Fig. 3a shows the shape of a 7 μl water droplet on the as-prepared surface. The equilibrium static CA is 153.8° ± 1.7°, demonstrating that the heterogeneous topographic surface overall presents superhydrophobicity. Fig. 3b and c show the time sequences of snapshots of a water droplet rolling along the 1 direction and the 2 direction, respectively. As can be seen, a 7 μl droplet starts to roll off the as-prepared surface along the 1 direction under the gravitation effect when the surface is slightly tilted at an angle of 56.5° (see Movie S2 in the ESI†). However, the droplet starts to roll along the 2 direction until the as-prepared surface is tilted 77.5° (see Movie S3 in the ESI†). The result demonstrates directional adhesive property on the superhydrophobic triangle array structure, that is, a droplet rolls along the 1 direction distinctly easier than its opposite direction (the 2 direction). Apparently, this anisotropy is attributed to the directional arrangement of triangle array patterns with the single axis of symmetry. The anisotropy at the one-dimensional level is similar to the superhydrophobic butterfly wings. When the as-prepared surface is tilted a angle between 56.5° and 77.5°, a 7 μl droplet will experience a slip behavior along the 1 direction but a pin behavior along the 2 direction. Thus the slippery-to-pinning property can be realized and the movement of a droplet can be controlled.

The directional adhesion of the triangle array patterned surfaces can be verified by measuring the contact angle hysteresis (CAH) as well. Fig. 4 shows the images of a droplet being dragged along the 1 and 2 directions, respectively (see Movie S4 in the ESI†). The advancing and receding angles along the 1 direction are about 150° and 92°. The advancing and receding angles along the 2 direction are about 155.5° and 84.5°. As a result, the CAH in the 1 direction is about 58°. However, the CAH is about 71° in the 2 direction, which is distinctly larger than that in the 1 direction, indicating that the droplet prefers to roll along the 1 direction.

The base length and vertex angle of the triangle array patterns, which are the most crucial structure parameters, have important effect on the superhydrophobicity and water adhesion of the as-prepared surfaces. Fig. 5a shows the relationship between the static CA and d when α is always 60°. Clearly, all the CAs are higher than 150°, indicating that the as-prepared surface shows stable superhydrophobic property in a wide d range from 0 μm to 1400 μm. The dependence of the SA on d is also investigated, as shown in Fig. 5b. When d is equal to 0 μm (the surface is completely irradiated by fs laser), the as-prepared surface shows ultralow water adhesion with SA lower than 1°. With the increase of d,

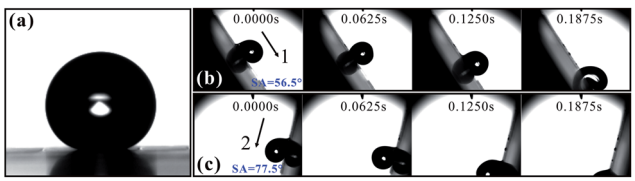

Fig. 3 The static and dynamic wettability of the periodic triangle array pattern with base length of 1200 μm and vertex angle of 60°. (a) The shape of a 7 μl water droplet on the surface with a contact angle of 153.8° ± 1.7°. (b and c) The time sequences of snapshots of a water droplet rolling along the 1 direction and the 2 direction. The as-prepared surface in (b) and (c) is tilted 56.5° and 77.5°, respectively.

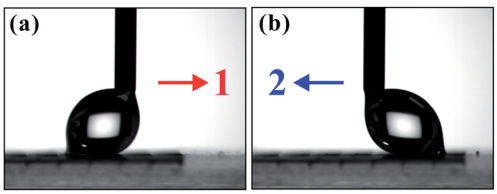

Fig. 4 Measurements of the advancing and receding angles on the triangle array patterned surface with base length of 1200 μm and vertex angle of 60° along the 1 (a) and 2 (b) directions, respectively. The advancing and receding angles along the 1 direction are about 150° and 92°. The advancing and receding angles along the 2 direction are about 155.5° and 84.5°.

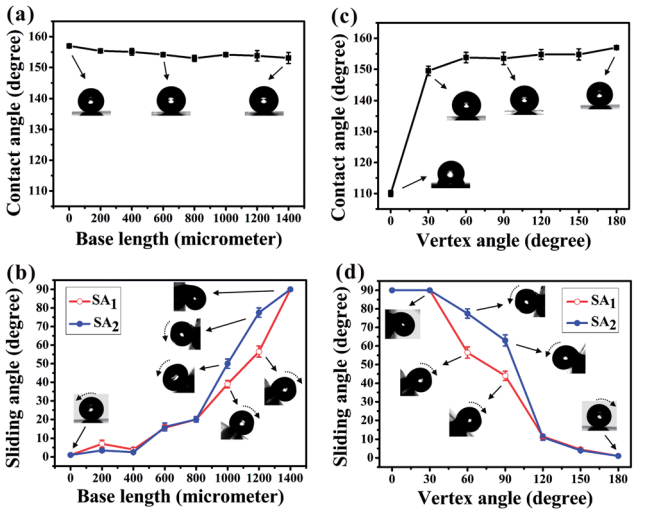

Fig. 5 The static and dynamic wettability of the periodic triangle array patterns as a function of the base length and vertex angle. (a and b) $\alpha \equiv 60°$; (c and d) $d \equiv 1200$ μm. The $d = 0$ μm for α being constant and $\alpha = 180°$ for d being constant mean that the surface is completely irradiated by a femtosecond laser. The $\alpha = 0°$ for d being constant means that the surface is intrinsic flat PDMS without any treatment.

the SA increases from ultralow to ultrahigh even when the as-prepared surfaces are 90° tilted in both the 1 and 2 directions. SA_1 and SA_2 have a similar trend. Subscripts 1 and 2 are for the 1 and 2 directions, respectively. When d increases from 0 μm to 800 μm, there is no significant difference between the SA_1 and the SA_2. At this time, the anisotropy does not display. However, the SA_1 is obvious smaller than the SA_2 when d is between 800 μm and 1400 μm, meaning that a droplet is easier to roll along the 1 direction than the 2 direction. Here the as-prepared surface shows superhydrophobicity and anisotropic adhesion in two opposite directions (at the one-dimensional level). On the other hand, the same conclusion can be obtained when α changes but the d remains constant at 1200 μm. The as-prepared surfaces show superhydrophobicity when α is equal to or greater than 30° (Fig. 5c). The SA_1 is obvious smaller than the SA_2 in a wide α range from 30° to 120°, showing anisotropic adhesion along the 1 and 2 directions (Fig. 5d). Specially, the maximum anisotropy reaches 21° at $d = 1200$ μm and $\alpha = 60°$.

It can be found that the anisotropy is obtained when the droplets have close size with a single hydrophobic triangle. As shown in Fig. 3a, the average diameter (≈1000 μm) of the contact area between the as-prepared surface and the 7 μl water droplet is almost the same as the height of a single triangle. At this point, the sliding anisotropy reaches a maximum. With the volume increasing from 7 μl to 20 μl, the sliding anisotropy declined from 21° to 9° and then to nearly 0°, resulting in anisotropic sliding disappearing, as shown in Fig. 6. In fact, this changing trend is consistent with the results of Fig. 5b. Increasing water volume for triangle size being constant is equivalent to decreasing triangle size for water volume being constant, because the two ways all make the size of the droplet become larger than the triangle.

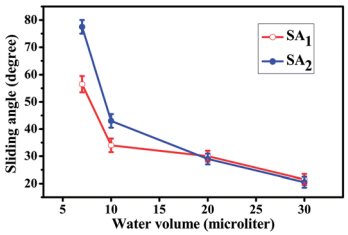

Fig. 6 Sliding angle as a function of water droplet volume on the triangle array patterned surface with base length of 1200 μm and vertex angle of 60°.

The three-phase contact line (TCL) of the location of water droplets is the main factor influencing the dynamic property of a droplet on the superhydrophobic surfaces.[37–40] In fact, it is known that the ordered arrangement of the microstructures may influence the contour, length and continuity of TCL and thus control the way a droplet tends to move.[3,41] TCL is similar in all directions for the homogeneous and random distribution of micropapillae on the surface of a lotus leaf, leading an isotropic wettability.[42,43] In comparison, on the surface of our as-prepared samples, the TCL which is influenced by the triangle array pattern seems more complex because the patterned surfaces are periodically heterogeneous. The completely laser-irradiated surface shows superhydrophobicity with ultralow water adhesion. Accordingly, the droplet on the laser-irradiated surface is Cassie state.[44,45] The water only contacts the peak of the micro/nanoscale hierarchical surface, leading an extremely discontinuous TCL. On the contrary, the droplet will wet the non-irradiated flat surface and form a continuous TCL. Therefore, a water droplet on the heterogeneous triangle array pattern generally composes of both discontinuous and continuous TCL. In addition, the edge of triangle array forms an energy barrier which can restrain and change the shape of TCL as well as the shape of the droplet.[17,28] The direction-dependent pattern has often resulted in a monosymmetric and irregular TCL shape, making the water droplet has different wetting situations when it will roll along different directions. For this reason, the anisotropic adhesion in the opposite directions of the as-prepared surface is ascribed to the direction-dependent arrangement of flat hydrophobic triangles surrounding by superhydrophobic rough structure.

Fig. 7 reveals the cause of the directional adhesion of the triangle array patterns. When the d of the triangle array pattern is small enough than the size of a water droplet, the droplet will contact tens or hundreds of single triangle. At this time, the pattern has relatively weak influence with the TCL shape for the statistical average effect. The shape of the TCL is close to circle on the horizontal sample or ellipse on the tilting sample, as shown in Fig. 7a and b. Now the triangle array pattern shows isotropic adhesion because the TCLs have similar situations when droplets will roll along the 1 and 2 directions. The completely laser-irradiated surface is a limiting isotropic case where the d goes to zero. A droplet on a surface with patterned superhydrophobic and intrinsic hydrophobic domains prefers to sit on top of the ordinary hydrophobic domains.[46] As the d

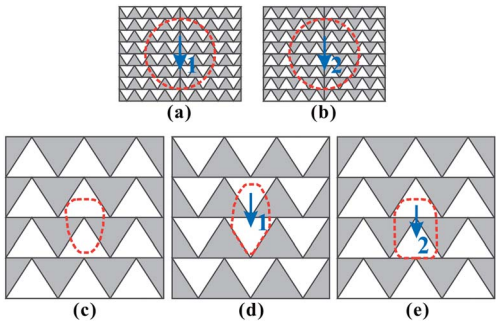

Fig. 7 Schematic illustration of the cause of the directional adhesion. (a and b) A droplet just rolling along the 1 (a) and 2 (b) directions, respectively, on the triangle array patterned surfaces with *d* being small enough than the size of the water droplet. (c–e) A droplet resting (c), just rolling along the1 (d) and 2 (e) directions, respectively, on the triangle array patterned surfaces with *d* having the same size as the droplet. The red dashed line shows the probable three-phase contact line.

increases, the effect of the triangle array pattern on the shape of the TCL becomes more prominent, especially when each single triangle is of the same size as the droplet. For example, when $d = 1200$ μm and $\alpha = 60°$, the difference of the SAs along the 1 and 2 directions can reach 21° for a 7 μl droplet. On such a surface, the TCL is not the circle, but an irregular shape (Fig. 7c). The pattern makes the water droplet have different TCL situation when it will roll along the 1 and 2 directions, as shown in Fig. 7d and e. In particular, the droplet suffers from the restriction arising from the base line of triangle (Fig. 7e) is strong than it arising from the bevel sides of isosceles triangle (Fig. 7d). As a result, a droplet rolls along the 1 direction distinctly easier than the 2 direction. The direction-dependent arrangement of flat hydrophobic triangles surrounding by superhydrophobic micro/nanoscale hierarchical structure ultimately produces directional anisotropic adhesion. The above analysis will offer important information for designing for direction-controllable wettability on a solid surface.

4. Conclusions

In summary, a kind of triangle array patterns showing superhydrophobicity and anisotropic adhesion at the one-dimensional level is demonstrated. On that surfaces, a droplet rolls along one direction obviously easier than its opposite direction. The anisotropy is obtained when the droplet is close to the size of a single hydrophobic triangle, and the maximum sliding anisotropy along two opposite directions can reach up to 21°. This unique ability is ascribed to the direction-dependent arrangement of hydrophobic triangle array surrounding by superhydrophobic domain. The pattern makes the TCL shape become irregular and the water droplet has different TCL situations when it will roll along two opposite directions, leading an directional anisotropic adhesion. This study not only presents a route for the fabrication of directional adhesive superhydrophobic surfaces but also provides insights into the nature, function, and design of the smart fluid-controllable interfaces. The anisotropic adhesive surfaces can be potentially applied in novel microfluidic devices and directional easy-cleaning coatings.

Acknowledgements

This work is supported by the National Science Foundation of China under the Grant no. 61275008, 51335008 and 61176113, the special-funded programme on national key scientific instruments and equipment development of China under the Grant no. 2012YQ12004706.

References

1 X. F. Gao and L. Jiang, *Nature*, 2004, **432**, 36.
2 D. L. Hu, B. Chan and J. W. M. Bush, *Nature*, 2003, **424**, 663.
3 Y. M. Zheng, X. F. Gao and L. Jiang, *Soft Matter*, 2007, **3**, 178.
4 J. Ju, H. Bai, Y. M. Zheng, T. Y. Zhao, R. C. Fang and L. Jiang, *Nat. Commun.*, 2012, **3**, 1247.
5 Y. M. Zheng, H. Bai, Z. B. Huang, X. L. Tian, F. Q. Nie, Y. Zhao, J. Zhai and L. Jiang, *Nature*, 2010, **463**, 640.
6 F. Xia and L. Jiang, *Adv. Mater.*, 2008, **20**, 2842.
7 B. Bhushan, *Philos. Trans. R. Soc., A*, 2009, **367**, 1445.
8 K. S. Liu and L. Jiang, *Nano Today*, 2011, **6**, 155.
9 Y. L. Zhang, Q. D. Chen, Z. Jin, E. Kim and H. B. Sun, *Nanoscale*, 2012, **4**, 4858.
10 L. Feng, S. H. Li, Y. S. Li, H. J. Li, L. J. Zhang, J. Zhai, Y. L. Song, B. Q. Liu, L. Jiang and D. B. Zhu, *Adv. Mater.*, 2002, **14**, 1857.
11 D. Wu, J. N. Wang, S. Z. Wu, Q. D. Chen, S. Zhao, H. Zhang, H. B. Sun and L. Jiang, *Adv. Funct. Mater.*, 2011, **21**, 2927.
12 J. Genzer and K. Efimenko, *Biofouling*, 2006, **22**, 339.
13 M. J. Hancock, K. Sekeroglu and M. C. Demirel, *Adv. Funct. Mater.*, 2012, **22**, 2223.
14 M. K. Kwak, H. E. Jeong, T. I. Kim, H. Yoon and K. Y. Suh, *Soft Matter*, 2010, **6**, 1849.
15 G. Lagubeau, M. L. Merrer, C. Clanet and D. Quéré, *Nat. Phys.*, 2011, **7**, 395.
16 M. Gleiche, L. F. Chi and H. Fuchs, *Nature*, 2000, **403**, 173.
17 F. Chen, D. S. Zhang, Q. Yang, X. H. Wang, B. J. Dai, X. M. Li, X. Q. Hao, Y. C. Ding, J. H. Si and X. Hou, *Langmuir*, 2011, **27**, 359.
18 E. Mele, S. Girardo and D. Pisignano, *Langmuir*, 2012, **28**, 5312.
19 H. S. Khoo and F. G. Tseng, *Appl. Phys. Lett.*, 2009, **95**, 063108.
20 N. A. Malvadkar, M. J. Hancock, K. Sekeroglu, W. J. Dressick and M. C. Demirel, *Nat. Mater.*, 2010, **9**, 1023.
21 P. Guo, Y. M. Zheng, C. C. Liu, J. Ju and L. Jiang, *Soft Matter*, 2012, **8**, 1770.
22 X. Yao, Y. L. Song and L. Jiang, *Adv. Mater.*, 2011, **23**, 719.
23 X. J. Liu, Y. M. Liang, F. Zhou and W. M. Liu, *Soft Matter*, 2012, **8**, 2070.
24 X. M. Li, D. Reinhoudt and M. Crego-Calama, *Chem. Soc. Rev.*, 2007, **36**, 1350.
25 Y. B. Zhang, Y. Chen, L. Shi, J. Li and Z. G. Guo, *J. Mater. Chem.*, 2012, **22**, 799.

26 Y. L. Zhang, H. Xia, E. Kim and H. B. Sun, *Soft Matter*, 2012, **8**, 11217.
27 F. Chen, D. S. Zhang, Q. Yang, J. L. Yong, G. Q. Du, J. H. Si, F. Yun and X. Hou, *ACS Appl. Mater. Interfaces*, 2013, **5**, 6777.
28 D. S. Zhang, F. Chen, Q. Yang, J. H. Si and X. Hou, *Soft Matter*, 2011, **7**, 8337.
29 F. Chen, H. W. Liu, Q. Yang, X. H. Wang, C. Hou, H. Bian, W. W. Liang, J. H. Si and X. Hou, *Opt. Express*, 2010, **18**, 20334.
30 S. G. He, F. Chen, K. Y. Liu, Q. Yang, H. W. Liu, H. Bian, X. W. Meng, C. Shan, J. H. Si, Y. L. Zhao and X. Hou, *Opt. Lett.*, 2012, **37**, 3825.
31 J. L. Yong, F. Chen, Q. Yang, D. S. Zhang, H. Bian, G. Q. Du, J. H. Si, X. W. Meng and X. Hou, *Langmuir*, 2013, **29**, 3274.
32 J. L. Yong, Q. Yang, F. Chen, D. S. Zhang, H. Bian, Y. Ou, J. H. Si, G. Q. Du and X. Hou, *Appl. Phys. A*, 2013, **111**, 243.
33 J. L. Yong, F. Chen, Q. Yang, G. Q. Du, H. Bian, D. S. Zhang, J. H. Si, F. Yun and X. Hou, *ACS Appl. Mater. Interfaces*, 2013, **5**, 9382.
34 D. S. Zhang, F. Chen, Q. Yang, J. L. Yong, H. Bian, Y. Ou, J. H. Si, X. W. Meng and X. Hou, *ACS Appl. Mater. Interfaces*, 2012, **4**, 4905.
35 J. L. Yong, F. Chen, Q. Yang, D. S. Zhang, G. Q. Du, J. H. Si, F. Yun and X. Hou, *J. Phys. Chem. C*, 2013, **117**, 24907.
36 J. L. Yong, Q. Yang, F. Chen, D. S. Zhang, G. Q. Du, H. Bian, J. H. Si, F. Yun and X. Hou, *Appl. Surf. Sci.*, 2014, **288**, 579–583.
37 X. D. Zhou, H. M. Fan, X. Y. Liu, H. Pan and H. Y. Xu, *Langmuir*, 2011, **27**, 3224.
38 L. Gao and T. J. McCarthy, *Langmuir*, 2007, **23**, 3762.
39 G. McHale, *Langmuir*, 2007, **23**, 8200.
40 H. Y. Erbil and C. E. Cansoy, *Langmuir*, 2009, **25**, 14135.
41 L. Gao and T. J. McCarthy, *Langmuir*, 2009, **25**, 7249.
42 W. Barthlott and C. Neinhuis, *Planta*, 1997, **202**, 1.
43 V. Zorba, E. Stratakis, M. Barberolou, E. Spanakis, P. Tzanetakis, S. H. Anastasiadis and C. Fotakis, *Adv. Mater.*, 2008, **20**, 4049.
44 A. B. D. Cassie and S. Baxter, *Trans. Faraday Soc.*, 1944, **40**, 546.
45 J. Li, X. H. Liu, Y. P. Ye, H. D. Zhou and J. M. Chen, *J. Phys. Chem. C*, 2011, **115**, 4726.
46 V. Jokinen, L. Sainiemi and S. Franssile, *Adv. Mater.*, 2008, **20**, 3453.